Spontaneous flux and magnetic-interference patterns in 0-π Josephson junctions

J. R. Kirtley
IBM T. J. Watson Research Center, P.O. Box 218, Yorktown Heights, New York 10598

K. A. Moler
Department of Physics, Princeton University, Princeton, New Jersey 08544

D. J. Scalapino
Department of Physics, University of California, Santa Barbara, California 93106

(Received 19 February 1997)

The spontaneous flux generation and magnetic field modulation of the critical current in a 0-π Josephson junction are calculated for different ratios of the junction length L to the Josephsen penetration depth λ_J, and different ratios of the 0-junction length to the π-junction length. These calculations apply to a Pb-$YBa_2Cu_3O_{7-\delta}$ (YBCO) c-axis-oriented junction with one YBCO twin boundary, as well as other experimental systems. Measurements of such a junction can provide information on the nature of the c-axis Josephson coupling and the symmetry of the order parameter in YBCO. We find spontaneous flux even for very short symmetric 0-π junctions, but asymmetric junctions have qualitatively different behavior. [S0163-1829(97)01726-8]

I. INTRODUCTION

Although many measurements now support the idea that the gap in the high-temperature cuprate superconductors has dominant $d_{x^2-y^2}$ character,[1] an orthorhombic superconductor such as $YBa_2Cu_3O_{7-\delta}$ (YBCO) cannot be described as a purely tetragonal d wave. In the orthorhombic symmetry group the d_{x^2-y2}- and s-wave basis functions belong to the same irreducible representation, so that one expects that the gap can be described as $d_{x^2-y^2}$ wave with some s-wave admixture, $d+\alpha s$. The deviation from purely d-wave behavior is supported by the observations[2,3] of Josephson pair tunneling from Pb into c-axis-oriented YBCO, although the variation of the Josephson tunneling strength with twin density, the relative areas of the twins, and the possible role of Josephson screening currents remain open questions.[4] It has also been proposed that these results can be explained by the development of a complex order parameter at twin boundaries[5] or mixing of states with s and $d_{x^2-y^2}$ symmetry at the Pb-YBCO interface.[6] Part of the problem of interpreting these experiments is the complex geometry presented by highly twinned materials. Here we consider the simpler case of a c-axis YBCO-Pb tunnel junction in which the YBCO has only one twin boundary in the junction. Experimental efforts on this system are currently underway.[7]

In the idealized geometry we describe below (Fig. 1), the Pb/YBCO junction which contains a single twin boundary can be described as a ''0-π'' junction, where the pair transfer integral has a relative pair phase of 0 in the left part of the junction (length L_0) and π in the right part of the junction (length L_π). Here we are interested in understanding the behavior of such 0-π Josephson junctions. While we describe our geometry in terms of c-axis tunneling in YBCO-Pb junctions, our results apply equally well to the 0-π a-b plane YBCO-Pb planar junctions[8] and grain boundary junctions[9,10] used for phase-sensitive tests of the symmetry of the high-T_c superconductors. In particular, while traditionally one considers the magnetic interference pattern, we will also be interested in spontaneous flux, flux generated by the self-screening Josephson currents in the absence of a drive current, and an external field H_e, which can be directly probed

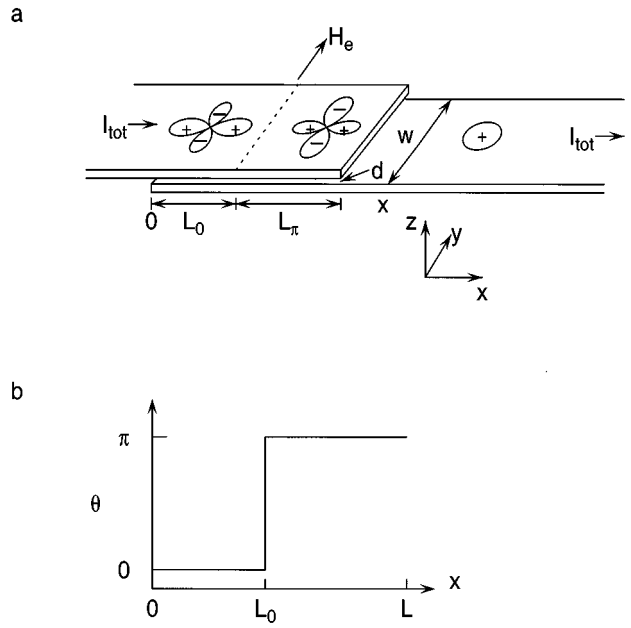

FIG. 1. (a) Junction geometry showing the directions of the external current flow I_{tot} and magnetic field H_e. The dashed line marks the twin boundary, and the gap functions are schematically illustrated such that the basic Josephson pair phase arising from the pair wave function overlap is 0 for $0<x<L_0$ and π for $L_0<x<L$. (b) Relative pair tunneling phase across the junction as a function of position.

by, for example, a scanning superconducting quantum interference device (SQUID) microscope.[9] As noted in Ref. 11, the two measurements are complementary, since while the magnetic field interference patterns are only strikingly different between a 0-π junction and a conventional 0-0 junction in the short junction limit $L \lesssim \lambda_J$, appreciable spontaneous flux only appears in the 0-π junction in the long junction limit $L \gtrsim \lambda_J$.

The maximum Josephson current I_c which a junction can carry versus an external magnetic field H_e applied parallel to the plane of the junction is called the ''magnetic interference pattern.'' The interference pattern for a short ($L \ll \lambda_J$) 0-π junction has been discussed by Wollman *et al.*[8] Xu *et al.*[11] have estimated the crossover to the limiting case of a long ($L \gg \lambda_J$) 0-π junction. With the approximations made by Xu *et al.*, the magnetically modulated critical current of a long 0-π junction is basically identical to the conventional 0-0 junction due to entrance of a half-flux quantum vortex, and the solution which contains spontaneously generated flux ceases to be a global minimum of the free energy for short junctions. Our exact numerical solutions, however, show that there is still a ''dip'' in the center of the diffraction patterns even for junctions as long as $10\lambda_J$, and that the symmetric junction should contain spontaneously generated magnetic flux even for $L < \lambda_J$. Here we are primarily interested in determining the behavior of a 0-π junction for intermediate values of L/λ_J and different L_0/L_π asymmetries. We believe that the dependence on L/λ_J of both the field-modulated critical current and the spontaneous flux generation of a Pb-YBCO junction with one twin boundary can provide important information on the c-axis coupling.

In the following, we discuss a numerical method for calculating the spontaneous flux generation and magnetic interference patterns for arbitrary junction lengths L/λ_J and junction asymmetries L_0/L_π. We then compare results for the critical current I_c versus external magnetic field H_e for the case of a traditional 0-0 junction with the symmetric 0-π case as a function of the reduced junction length L/λ_J. Following this, we focus on the Josephson screening currents by examining the flux generated by these self-currents in the absence of an external current and magnetic field. As previously noted, this self-generated flux can be probed using a scanning SQUID microscope,[9] providing important information on the nature of the c-axis Josephson coupling. We then turn to the interesting case in which the areas of the two twin regions differ and again look at the self-flux versus L/λ_J. There is a qualitative difference between the results for the spontaneous flux generation which occurs in asymmetric junctions compared to symmetric junctions. We show briefly how these results can be extended to a junction with multiple twin boundaries. We conclude by discussing what this type of experiment can tell us about the Pb-YBCO c-axis Josephson tunneling.

II. CALCULATION

The geometry and gap structure which we envision is illustrated in Fig. 1. In this idealized geometry,[12] the upper YBCO strip contains a twin boundary which separates the YBCO-Pb junction into two regions. As schematically illustrated in Fig. 1, we have taken the phase of the larger lobe of the $d+\alpha s$ gap in region $0<x<L_0$ to be positive. Then, if the phase is locked across the grain boundary as one expects,[13] the larger lobe in region $L_0<x<L$ will be negative. Thus the pair transfer integral between the YBCO and the Pb leads to a relative Josephson pair phase of 0 for $0<x<L_0$ and π for $L_0<x<L$.

Following the notation of Owen and Scalapino,[12] we describe a junction (Fig. 1) with width w small compared to λ_J in the y direction, of length L in the x direction, carrying a total current $I_{\rm tot}$ in the x direction, in an external magnetic field H_e oriented in the y direction. We include the effects of the 0 and π junctions by introducing an extra phase angle $\theta(x)$ which takes the value 0 or π. The superconducting phase difference across the junction is then just the solution of the sine-Gordon equation

$$\frac{\partial^2\phi}{\partial x^2}=\frac{1}{\lambda_J^2}\sin[\phi(x)+\theta(x)]. \tag{2.1}$$

Applying Ampère's law with a contour of integration around the perimeter of the junction in the xy plane leads to the boundary condition

$$H(L)-H(0)=4\pi I_{\rm tot}/cw. \tag{2.2}$$

Contours of integration in the yz plane circling the leads at $x=0$ and $x=L$ lead to

$$H(L)+H(0)=2H_e. \tag{2.3}$$

The Josephson penetration depth is given by

$$\lambda_J=\left(\frac{\hbar c^2}{8\pi e d j_c}\right)^{1/2}, \tag{2.4}$$

where d is the sum of the Pb and YBCO λ_{ab} penetration depths plus the thickness of the insulator layer between the two superconductors, and j_c is the Josephson critical current density. The current per unit length through the junction is given by

$$j(x)=wj_c\sin[\phi(x)+\theta(x)]. \tag{2.5}$$

The gradient of the phase is in turn related to the field H in the junction by

$$H(x)=\frac{\hbar c}{2ed}\frac{\partial\phi}{\partial x}. \tag{2.6}$$

If we redefine the parameters $H(x)$ and $I_{\rm tot}$ as

$$h(x)=\frac{2ed\lambda_J}{\hbar c}H(x)=\lambda_J\frac{\partial\phi}{\partial x} \tag{2.7}$$

and

$$i_{\rm tot}=\frac{I_{\rm tot}}{2\lambda_J w j_c}, \tag{2.8}$$

the boundary conditions become

$$h(L)=i_{\rm tot}+h_e, \tag{2.9}$$

$$h(0)=-i_{\rm tot}+h_e. \tag{2.10}$$

Defining a dimensionless coupling parameter

$$\alpha = \frac{\lambda_J^2}{(\Delta x)^2}, \tag{2.11}$$

the differential equation turns into a difference equation on a grid of size Δx:

$$\phi_{n+1} - 2\phi_n + \phi_{n-1} = \frac{1}{\alpha}\sin(\phi_n + \theta_n). \tag{2.12}$$

The boundary conditions are then described as difference equations, where n_j is the total number of junctions:

$$\phi_{n_j} - \phi_{n_j - 1} = \frac{i_{\rm tot} + h_e}{\sqrt{\alpha}}, \tag{2.13}$$

$$\phi_2 - \phi_1 = \frac{-i_{\rm tot} + h_e}{\sqrt{\alpha}}. \tag{2.14}$$

These coupled difference equations are solved using a relaxation method to find the solution $\phi(x)$. The free energy of this solution is given by

$$F = \frac{\hbar j_c w}{2e}\int_{-L/2}^{L/2}\left[1 - \cos[\phi(x) + \theta(x)] + \frac{\lambda_J^2}{2}\left(\frac{\partial \phi}{\partial x}\right)^2\right]dx. \tag{2.15}$$

Written as a difference equation, the free energy for the vortex solution becomes

$$F_V = \frac{\hbar j_c w \Delta x}{2e}\sum_1^{n_j - 1}\left(1 - \cos(\phi_n + \theta_n) + \frac{\alpha}{2}(\phi_{n+1} - \phi_n)^2\right), \tag{2.16}$$

while the free energy of the no-vortex ($\phi = 0$ everywhere) solution is

$$F_0 = \frac{\hbar j_c w \Delta x}{2e}\sum_1^{n_j - 1}(1 - \cos\theta_n). \tag{2.17}$$

To obtain the critical current, the current $I_{\rm tot}$ through the junction is increased in steps, iterating the solution until either the convergence criterion

$$\epsilon > \left\{\left[[\phi_1 - \phi_2 - (i - h_e)/\alpha^{1/2}]^2 + [\phi_{n_j} - \phi_{n_{j-1}} - (i + h_e)/\alpha^{1/2}]^2 + \sum_{n=2}^{n_j - 1}[\phi_{n+1} + \phi_{n-1} - 2\phi_n - \sin(\phi_n + \theta_n)/\alpha]^2\right]/n_j\right\}^{1/2} \Big/ \pi \tag{2.18}$$

is satisfied, with ϵ normally chosen to be 10^{-6}, or until the solution diverges with $|\phi(n_j/2)| > 25$. For particular values of the parameters, we compare solutions with ϵ taken to be 10^{-6}, 10^{-7}, and 10^{-8} to check the convergence of the solution. The largest value of $I_{\rm tot}$ for which the iterations converge is taken to be the critical current I_c. For the numerical calculations shown in the next section, we took $L = 10$, $\Delta x = 0.1$, and $n_j = L/\Delta x = 100$, which meant that the dimensionless coupling constant ranged from $\alpha = 10^4$ for $L/\lambda_J = 1$ to $\alpha = 10^2$ for $L/\lambda_J = 10$: Δx was always much smaller than L_0, L_π, or λ_J.

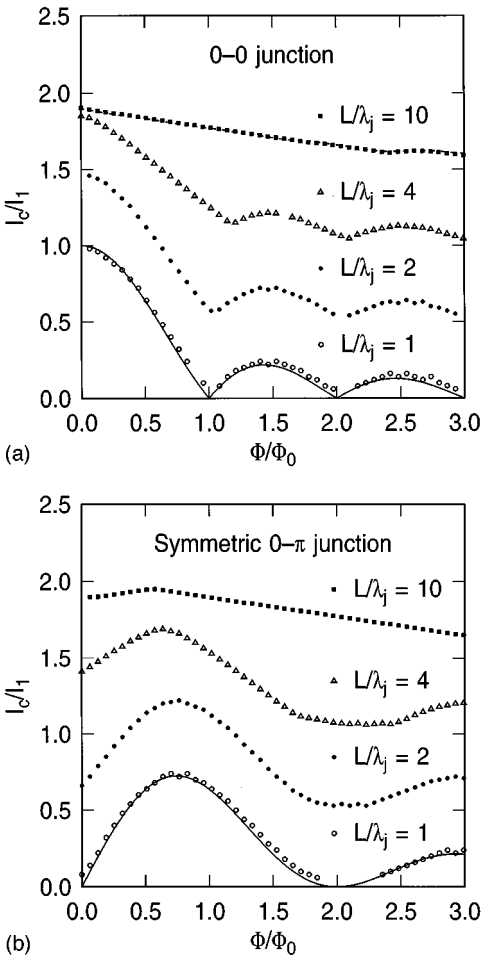

FIG. 2. The dependence of the junction critical current I_c/I_1 as a function of the field in the junction Φ/Φ_0, for a series of junction lengths L/λ_J, for a 0-0 junction (a) and a symmetric 0-π junction (b). The solid curve is the analytical result in the short junction $L \ll \lambda_J$ limit. The dashed curve in (a) is the result for $L/\lambda_J = 10$ from Ref. 12. Curves for successive values of L/λ_J have been offset vertically by 0.5 units for clarity.

III. RESULTS

Figure 2 compares our results for the magnetic interference pattern for a 0-0 junction (a) and a symmetric 0-π junction (b) for various values of the reduced length L/λ_J. Here we have plotted I_c/I_1 versus Φ/Φ_0, where $I_1 = j_c w L$, $\Phi = H_e d L$, and $\Phi_0 = hc/2e$ is the superconducting flux quantum. In the short junction limit $L \ll \lambda_J$, the critical current can be written as

$$I_c(B) = \frac{I_1}{L}\max\left[\int_0^L \sin\left(\frac{2\pi H_e x d}{\Phi_0} + \theta(x) + \psi\right)dx\right], \tag{3.1}$$

where $\theta(x)$ can be 0 or π, and the maximum value of the expression is obtained by varying $0 < \psi < 2\pi$ for each value of H_e. For the 0-0 junction [$\theta(x) = 0$] this expression reduces to

$$\frac{I_c}{I_1}=\frac{|\sin(\pi\Phi/\Phi_0)|}{|\pi\Phi/\Phi_0|}, \tag{3.2}$$

while for the symmetric 0-π junction $[\theta(x)=0, x<L/2; \theta(x)=\pi, x\geq L/2]$ this becomes

$$\frac{I_c}{I_1}=\frac{\sin^2(\pi\Phi/2\Phi_0)}{|\pi\Phi/2\Phi_0|}. \tag{3.3}$$

These equations are plotted as the solid lines in Fig. 2. Also included in Fig. 2(a) is the result of Owen and Scalapino for the reduced length $L/\lambda_J=10$. For the 0-0 junction the effect of increasing L is to reduce the height of the central peak in the magnetic interference pattern and to reduce the amplitude of the successive oscillations as H_e is increased. For the 0-π junction, increasing L tends to reduce the depth of the minimum at $H_e=0$, and as $L/\lambda_J\rightarrow\infty$ the curves for the 0-0 junction and the 0-π junction become identical as discussed by Xu *et al.*[11] However, even for $L/\lambda_J=10$, we find, as shown in Fig. 2(b), that the critical current initially increases with flux until $\Phi/\Phi_0\cong 0.5$. This differs from the $L/\lambda_J=10$ result shown in Ref. 11. We believe that this difference results from the approximation made by Xu *et al.* that the presence of a π vortex simply changes the phase in the π section of the junction by π, effectively changing it into a 0 junction. This approximation is valid on length scales large compared to λ_J, but, as shown in Fig. 2(b), leads to an experimentally detectable difference in the solutions even for L as long as $10\lambda_J$. For short- and medium-length junctions, Xu *et al.* took the analytical long-junction expression and made the approximation that the effect of shortening the junction would be simply to cut off this expression. However, this is not a valid solution of the modified sine-Gordon equation and the boundary conditions. It also leads, as we show below, to dramatic differences in both the free energy and the total flux for the π-vortex solutions for short- to medium-length junctions.

Figure 3 addresses the question of spontaneous flux generation in 0-π junctions as a function of reduced length L/λ_J and the degree of asymmetry (L_π/L). Figure 3(a) plots the ratio of the free energy of the state with some spontaneous flux to the state with no flux. The dashed line is the result of Xu *et al.*, using the approximation outlined above. The solid lines are our full results. Note that, in contrast to the results of Xu *et al.*, for the symmetric 0-π junction $(L_\pi/L=0.5)$ the state with spontaneous flux always has lower energy than the state with no flux, and thus some self-generated flux should therefore be present for all values of L/λ_J. Figure 3(b) plots the spontaneous flux vs L_π/λ_J. The inset in this figure shows that the spontaneous flux for a symmetric junction follows a power law dependence on junction length for short junctions. In this limit the phase ϕ has only small deviations from an average value of $\pi/2$, and the spontaneously generated field increases linearly towards the center of the junction from a value of zero at the edges. A simple geometrical argument, expanding the sine-Gordon equation about $\phi=\pi/2$, implies that for short junctions the spontaneous flux should be given by $\Phi/\Phi_0=(L/\lambda_J)^2/8\pi$. This relation is plotted as a straight line in the inset of Fig. 3(b). However, for the asymmetric case, the state with no flux has the lowest free energy for short

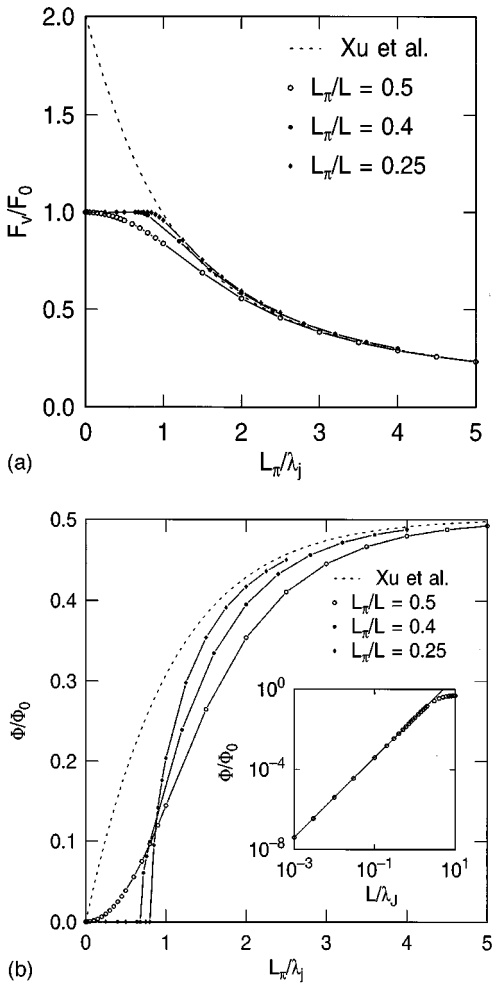

FIG. 3. The ratio of the free energy for the solution with spontaneous flux F_v to that with no flux F_0 (a) and the spontaneous total flux in the junction Φ/Φ_0 (b), for a 0-π junction as a function of the length of the π junction L_π/λ_J, for different asymmetries L_π/L. The inset of (b) shows the results for a symmetric junction on a log-log scale. The straight line is the relation $\Phi/\Phi_0=(L/\lambda_J)^2/8\pi$.

junctions, and as shown in Fig. 3(b), there is no spontaneously generated flux, up to a critical value of $L_\pi/\lambda_J\lesssim 1$. The amount of spontaneously generated flux approaches $\Phi_0/2$ as L_π gets larger, and rate of increase of flux at the onset of flux generation increases for less symmetrical junctions.

The onset of spontaneous flux generation is also apparent in the magnetic interference patterns, as shown in Fig. 4. Here we hold the asymmetry factor L_π/L fixed at 0.25, and vary the length of the junction L_π/λ_J. For small L_π/λ_J there is no spontaneous flux generated, and the magnetic interference has a minimum at zero field. However, as L_π/λ_J approaches unity, there is an abrupt shift to a magnetic interference pattern with a maximum at zero field. The solid line in Fig. 4 is the short-junction limit calculated from Eq. (3.1), which is a good indicator of the actual interference pattern only until flux generation becomes energetically favorable.

The behavior of junctions with multiple twin boundaries can be calculated using the same techniques, as long as the junction width w is small compared to λ_J. We show the

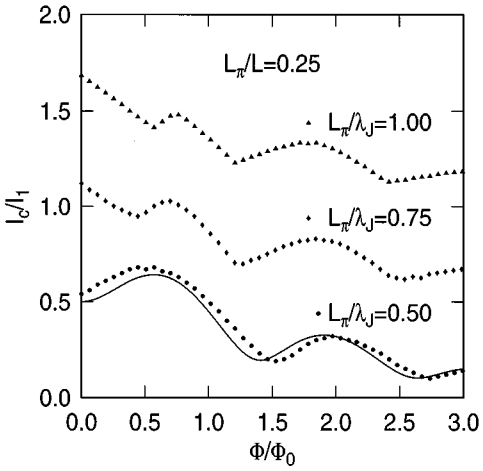

FIG. 4. The dependence of the critical current I_c/I_1 as a function of field in the junction Φ/Φ_0, for a junction with asymmetry $L_\pi/L=0.25$, for three different junction lengths: $L_\pi/\lambda_J=0.5$, well below the critical length for spontaneous flux generation; $L_\pi/\lambda_J=0.75$, near the critical length; and $L_\pi/\lambda_J=1$, above the critical length. The solid curve is calculated using the short junction approximation, Eq. (3.1). Curves for successive values of L/λ_J have been offset vertically by 0.5 units for clarity.

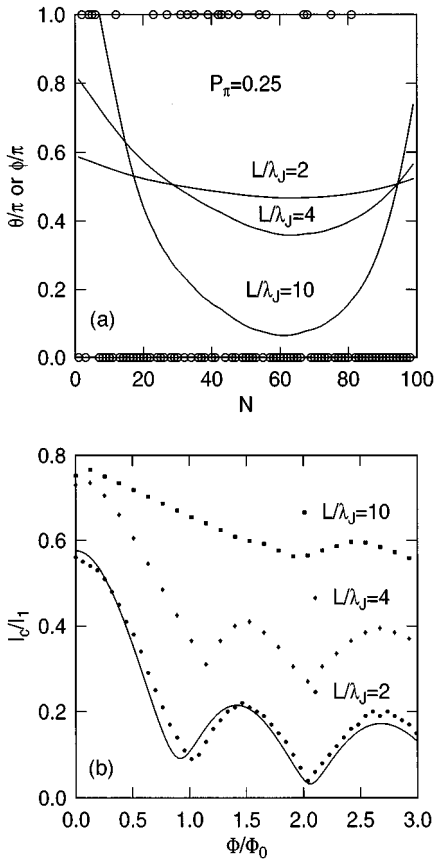

FIG. 5. (a) The circles show 100 randomly distributed 0 and π phases, assuming a probability of π phase$=0.25$. The solid lines show the solutions for ϕ at $I=I_c$ and $H_e=0$. (b) The solid curve is the magnetic interference pattern for a junction with this distribution of phases in the short junction limit, Eq. (3.1). The solid points are the result of the full numerical calculation for various values of L/λ_J. Successive L/λ_J curves have been offset vertically by 0.2 units for clarity.

results of one such set of calculations in Fig. 5. Here we have assumed that there are 100 twins in the junction, with the probability of a particular twin having 0 or π phase randomly distributed with the probability of π being 0.25. The circles in Fig. 5(a) show the randomly distributed set of 0 and π phases used in this calculation. The solid lines in Fig. 5(a) show the solution for the phase angle ϕ at $H_e=0$ and $I=I_c$, for various values of L/λ_J. These curves show, as expected, that the gradient of ϕ, and therefore the flux penetration into the junction, is spread throughout the junction for small L/λ_J, but is localized at the junction edges for $L/\lambda_J \gg 1$. The solid line in Fig. 5(b) shows the predicted interference pattern from Eq. (3.1) in the short-junction limit. The other symbols show the result of the full numerical solution for $L/\lambda_J=2$, 4, and 10. Even for this small number of randomly distributed twins, the interference pattern, although reduced in critical current, is similar to that for a single 0 junction [Fig. 2(a)] especially for larger values of L/λ_J. This figure shows how important it is that complete knowledge of the distribution of twins be available for the correct interpretation of experimental work on c-axis tunneling from twinned samples.

IV. CONCLUSION

As discussed by Sun *et al.*,[2] the results of their Pb-YBCO c-axis Josephson tunneling experiments can be interpreted as showing that the order parameter in YBCO must have some s-wave component. While this could be consistent with an order parameter having $d_{x^2-y^2}+\alpha s$ symmetry in an orthorhombic material, the interpretation of the experiments done on twinned materials depend on details of the multitwinned geometry. Here we have analyzed a simpler situation involving a single twin boundary. In this case, if the $d_{x^2-y^2}$ contribution is dominant, giving the type of order parameters illustrated in Fig. 1, one should observe the behavior we have discussed. In particular, if the junction areas for the two twin regions are equal, one has the conventional minimum in the critical current at zero magnetic field as shown in Fig. 2(b), if L/λ_J is sufficiently small, and provided the current density is uniform on a scale set by λ_J. For the asymmetric case in which the areas of the two twin regions differ, more striking behavior should appear. There should be a sudden shift of the interference pattern from one with a minimum at zero field, to one with a maximum (Fig. 4), as L_π/λ_J goes through unity. One way to vary L/λ_J would be by changing λ_J with temperature. Another would be to apply a magnetic field H_x to vary $\lambda_J(H_x)=\{\hbar c^2/[8\pi e d I(H_x)/wL]\}^{1/2}$, with $I(H_x)=I_1|\sin(\pi\Phi_x/\Phi_0)|/|\pi\Phi_x/\Phi_0|$, and $\Phi_x=H_x dw$. Alternatively, or in addition, one could use a scanning SQUID microscope to measure the spontaneous flux generated by the self-screening Josephson currents. For the case of equal areas, this spontaneous flux rises continuously as L_π/λ_J increases. However, for nonequal areas one finds no spontaneous flux generation below a critical value of $L_\pi/\lambda_J \sim 1$ and then a sharp increase in flux should occur. We believe that if these types of behavior are observed, they would show that the Pb-YBCO c-axis Josephson coupling is consistent with a description of the high T_c superconductors as having dominant $d_{x^2-y^2}$ symmetry.

ACKNOWLEDGMENTS

We would like to thank J. Clarke, R. C. Dynes, and A. G. Sun for interesting discussions of their experiments prior to publication, and S. Bahcall for a careful reading of the manuscript. D.J.S. acknowledges the National Science Foundation under Grant No. DMR95-27304.

[1] D. J. Scalapino, Phys. Rep. **250**, 329 (1995); J. F. Annett, N. Goldenfeld, and A. J. Leggett, J. Low Temp. Phys. **105**, 473 (1996), and references therein.

[2] A. G. Sun, D. A. Gajewski, M. B. Maple, and R. C. Dynes, Phys. Rev. Lett. **72**, 2267 (1994); A. S. Katz, A. G. Sun, and R. C. Dynes, Appl. Phys. Lett. **66**, 105 (1995).

[3] R. Kleiner *et al.*, Phys. Rev. Lett. **76**, 2161 (1996).

[4] C. O'Donovan , D. Branch, J. P. Carbotte, and J. S. Preston, Phys. Rev. B **51**, 6588 (1995); C. O'Donovan, M. D. Lumsden, B. D. Gaulin, and J. P. Carbotte (unpublished).

[5] M. Sigrist *et al.*, Phys. Rev. B **53**, 2835 (1996).

[6] S. R. Bahcall, Phys. Rev. Lett. **76**, 3634 (1996).

[7] J. Clarke, K. Kouznetsov, E. Chen, and A. G. Sun (private communication).

[8] D. A. Wollman *et al.*, Phys. Rev. Lett. **74**, 797 (1995); D. J. van Harlingen, Rev. Mod. Phys. **67**, 515 (1995).

[9] J. R. Kirtley *et al.*, Phys. Rev. Lett. **76**, 1336 (1996).

[10] J. H. Miller, Jr. *et al.*, Phys. Rev. Lett. **74**, 2347 (1995).

[11] J. H. Xu, J. H. Miller, and C. S. Ting, Phys. Rev. B **51**, 11 958 (1995).

[12] C. S. Owen and D. J. Scalapino, Phys. Rev. **164**, 538 (1967).

[13] M. B. Walker and J. Luettmer-Strathmann, Phys. Rev. B **54**, 588 (1996).